JOURNAL OF MATERIALS SCIENCE 17 (1982) 533–546

Carbazolyl and anthryl substituted diacetylenes: studies of crystal structures and energy transfer in the polymerization of mixed crystals

V. ENKELMANN, G. SCHLEIER
Institut für Makromolekulare Chemie, Hermann Staudinger Haus, Stefan-Meier Strasse 31, D-7800 Freiburg, West Germany

H. EICHELE
Lehrstuhl für Experimentalphysik II, Universität Bayreuth, D-8580 Bayreuth, West Germany

Diacetylenes substituted with carbazole and anthracene side groups can be co-crystallized to form substitutional solid solutions. By solid-state polymerization of these mixed crystals, macroscopic single crystals of the corresponding co-polymers are obtained. The crystal structures of the monomers are discussed with regard to structural aspects of the formation of solid solutions and the reactivity in the solid state. The influence of isostructural doping on the polymerization and the energy transfer involved in the reaction are discussed.

1. Introduction

1,4-substituted butadiynes (diacetylenes) are known to polymerize in the solid state. Due to the special mechanism of this topochemical polymerization, macroscopic, nearly defect-free, single crystals of polymer can be obtained. The polymerization is initiated thermally, or by irradiation, and leads to a planar, fully conjugated polymer chain by 1,4 additions of neighbouring monomer units according to

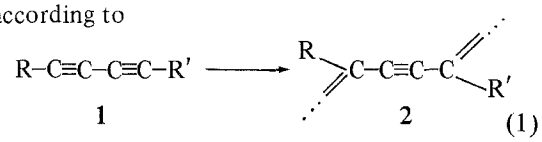

1 2 (1)

A polymerizing crystal can be described as a solid solution of polymer chains growing in the monomer lattice. Although there is normally a quite large mismatch between monomer and polymer lattices in many cases, no phase separation occurs and the monomer crystal is gradually transformed into the isomorphous polymer single crystal [1, 2].

For a large number of polydiacetylenes with different side groups, crystal structures and physical properties have been investigated, and the relationships between monomer packing and the reactivity and the nature of the reactive intermediates are well understood [3–10]. However, there are still open questions such as the energy transfer during polymerization, the quantitative description of the polymerization kinetics, or the influence of crystal perfection and the reaction conditions on the molecular weight and the molecular weight distribution of the polymers. Further insight into these problems can be obtained by studies of mixed crystal systems. Apart from the preparative aspect, i.e. diacetylene co-polymers can only be obtained from the corresponding monomer mixed crystals, they are of interest because co-monomer units introduced into the host lattice could be used as specific, well defined defects which vary the reactivity of the polymer, or as probes for the investigation of the complex energy transfer phenomena observed in the polymerization process.

In a previous study [11, 12] a series of mixed

0022–2461/82/020533–14$3.40/0

TABLE I The different monomers used in this work*.

Co-monomer	R	R'	Abbreviation
1a	$-CH_2-Cz$	$-CH_2-Cz$	DCH
1b	$-CH_2-A$	$-CH_2-A$	DAH
1c	$-CH_2-Cz$	$-CH_2-A$	ACH

*Cz represents a Carbazolyl group, A represents an Anthryl group.

crystals of bis(arylsulphonate) diacetylenes

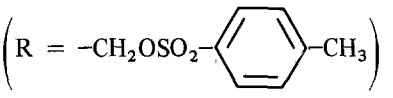

have been investigated. It was found that in this system, mixed crystals were formed only in a limited concentration range. In this range the induction period, which is typical for the thermal polymerization of these types of monomer, could be influenced whereas the activation energy remained unchanged. Recently Bloor *et al.* [13] have reported similar results for some other systems.

In this paper the preparation, polymerization and structural properties of mixed crystals formed from a series of diacetylene monomers with aromatic side groups will be described.

The Co-monomers 1a, 1b and 1c (see Table I) were chosen because Co-monomer 1a (1,6bis(N-carbazolyl)2,4-hexadiyne, DCH) is a well characterized monomer with interesting optical, structural and electrical properties, and because preliminary studies had indicated that here true solid solutions could be formed [14].

2. Experimental results

2.1. Preparation, characterization and polymerization

The co-monomers used for this work are listed in Table I. Co-monomers 1a, 1b, were prepared as described in previous literature as were Compounds 3 and 5 [N-(2-propynyl)-carbazole] [15–17]. The unsymmetrically substituted ACH, Co-monomer 1c, was obtained by the Chadiot–Chodkiewicz coupling reaction (see Section 2.1.2.) according to

$$\underset{3}{A-CH_2-C\equiv CH} + \underset{4}{BrC\equiv C-CH_2-Cz} \xrightarrow{CuCl} \underset{1c}{A-CH_2-C\equiv C-C\equiv C-CH_2-Cz} + HBr \quad (2)$$

Compound 4 was prepared as in Section 2.1.1.

Mixed crystals were obtained by passing a slow stream of methanol saturated nitrogen over the surface of concentrated solutions of the co-monomers in dimethylformamide (DMF). The composition of mixed crystals was determined by measuring the anthracene absorption at 389 nm in CH_2Cl_2 [18]. The polymerization was carried out by irradiation using a ^{60}Co γ-source with a dosage of 0.5 Mrad h^{-1}. The conversion was determined gravimetrically by extraction of residual monomer with DMF. The experimental set-up used to record the luminescence spectra of the crystals has been described previously [15, 19].

2.1.1. Preparation of N-(3-bromo-2-propynyl)-carbazole, Compound 4

To a solution of 32 g NaOH and 52 g Br_2 in 160 ml water, 41 g N-(2-propynyl)-carbazole (5) dissolved in 300 ml 1,2-dimethoxyethane was added. The mixture was stirred for 4 hours under nitrogen at room temperature. Then 200 ml water were added and the product was extracted with ether and crystallized from $CHCl_3$ (yield 67%, M.P. 127° C).

2.1.2. Preparation of ACH, Co-monomer 1c

8 g of Compound 3 were dissolved in 40 ml dimethylformamide (DMF) and a solution of 50 mg CuCl, 150 mg NH_3OHCl and 2.5 ml $EtNH_2$ in 10 ml of ethanol was added. 5.5 g of Compound 4, dissolved in a mixture of 15 ml DMF and 10 ml ethanol, were added slowly at a temperature of 30 to 35° C and the mixture was stirred for 2 hours at room temperature. The product was precipitated with water and crystallized from toluene (yield 30%).

2.2. Structure determination

The unit cell dimensions of single crystals were determined from Straumanis-type double radius Weissenberg photographs (R = 57.3 mm, where R is the radius of the camera) for Co-monomers 1a and 1b, and for Co-monomer 1c, from least-squares analyses of the setting angles of 15 centered reflections. The lattice dimensions of mixed crystals were obtained from single crystals as described before or from least-squares analyses of the d-values measured on Guinier photographs of powder samples. For Co-monomers 1a and 1b intensities were recorded by multiple-film equi-inclination Weissenberg photographs with Ni-filtered CuKα radiation. For the determination of

TABLE II Details of the structure determinations and refinements

Parameter	Co-monomer			
	1a	1a	1b	1c
Temperature (K)	300	120	300	300
Radiation	CuKα	CuKα	CuKα	MoKα
Number of reflections	596	417	701	3444
Observed reflections	459	397	608	1480
Unobserved reflections	137	15	93	1964
Intensity determination	film	film	film	counter
Refinement of C and N	isotropic	isotropic	anisotropic	anisotropic
Refinement of H	no	no	positions	positions
Final R index	0.13	0.13	0.098	0.09

the low temperature structure of DCH the temperature was maintained at 120 ± 3 K by means of a low temperature attachment.

The intensities, I, were estimated visually by comparison with a series of timed exposures of a selected reflection. Reflections having intensities less than the threshold value were assigned half the threshold value of the observable intensity and were given zero weight during the refinement. The scale factors for the different data sets were allowed to vary in the refinement. No absorption correction was applied. For ACH (Co-monomer 1c) intensities were collected with a crystal measuring 0.1 mm by 0.2 mm by 0.6 mm on a Nonius CAD 4 four circle diffractometer with graphite monochromated MoKα radiation. The $\theta - 2\theta$ scan mode was used. Reflections with $I < 2\sigma(I)$ were considered unobserved (where σ is the standard error).

The structures were solved by direct methods using the program MULTAN [20]. Refinement was done by full matrix least-squares analyses. Unit weights were used throughout the refinements. In DAH (Co-monomer 1b) and ACH the co-ordinates of the hydrogen atoms were found in difference maps. With DCH, fragmentation of the crystals at the phase transition was found to be a major difficulty, so that the low temperature structure intensities were recorded only for the $h\,0\,l$ and $h\,1\,l$ layers. Here the hydrogen atoms were assigned physically reasonable values and their contributions were included in structure factor calculations. The details of the structure determinations and refinements are summarized in Table II. The programs used were those of the XRAY76 system [21]. Scattering factors for C and N were taken from the International Tables for X-ray Crystallography [22] and for H from Stewart *et al.* [23]. Final atomic parameters are listed in Table III.*

TABLE IIIA Final atomic parameters for Co-monomer 1a at 300 K. Estimated standard deviations are given in parentheses

Atom	Fractional co-ordinates (×10⁴)			Isotropic temperature factor, B (nm²)
	x	y	z	
C (1)	9647 (15)	9280 (46)	9751 (11)	0.0515 (53)
C (2)	9083 (14)	7955 (46)	0371 (11)	0.0501 (52)
C (3)	8329 (14)	6272 (47)	8860 (10)	0.0516 (51)
C (4)	8010 (14)	9191 (44)	7617 (10)	0.0423 (49)
C (5)	7254 (14)	11142 (43)	7396 (11)	0.0414 (47)
C (6)	7275 (17)	12319 (52)	6611 (14)	0.0710 (62)
C (7)	7999 (18)	11165 (54)	6223 (12)	0.0682 (62)
C (8)	8718 (18)	9446 (57)	6447 (14)	0.0793 (69)
C (9)	8759 (16)	9446 (57)	7182 (12)	0.0582 (56)
C (10)	6986 (13)	9945 (42)	8600 (10)	0.0405 (47)
C (11)	6629 (15)	11751 (44)	7987 (11)	0.0442 (48)
C (12)	4764 (18)	13648 (56)	8058 (14)	0.0783 (70)
C (13)	5430 (19)	13603 (66)	8726 (17)	0.0912 (81)
C (14)	5725 (19)	11963 (62)	9341 (14)	0.0828 (72)
C (15)	6540 (17)	10124 (51)	9302 (12)	0.0641 (60)
N	7784 (11)	8427 (35)	8367 (8)	0.0434 (38)

*Lists of observed and calculated structure factors can be obtained upon request from V. Enkelmann.

TABLE IIIB Final atomic parameters for 1a at 120 K. Estimated standard deviations are given in parentheses

Atom	Fractional co-ordinates ($\times 10^4$)			Isotropic temperature factor, B (nm^2)
	x	y	z	
C (1)	245 (12)	712 (65)	279 (8)	0.0362 (43)
C (2)	700 (13)	2163 (75)	783 (9)	0.0385 (46)
C (3)	1247 (13)	4180 (76)	1337 (10)	0.0431 (46)
C (4)	2816 (14)	545 (72)	1411 (10)	0.0435 (47)
C (5)	3406 (12)	−1152 (73)	1935 (9)	0.0330 (41)
C (6)	4273 (13)	−2575 (70)	1722 (9)	0.0413 (46)
C (7)	4533 (13)	−2613 (70)	1037 (10)	0.0428 (47)
C (8)	3954 (13)	−955 (77)	522 (9)	0.0407 (46)
C (9)	3112 (14)	569 (73)	679 (10)	0.0499 (52)
C (10)	2036 (13)	1169 (76)	2436 (9)	0.0407 (47)
C (11)	2888 (13)	−696 (74)	2436 (9)	0.0413 (46)
C (12)	3078 (12)	−1763 (73)	3305 (9)	0.0411 (47)
C (13)	2419 (13)	−1037 (76)	3838 (9)	0.0359 (43)
C (14)	1595 (16)	867 (71)	3650 (11)	0.0563 (55)
C (15)	1368 (78)	2104 (10)	2966 (54)	0.0483 (54)
N	1990 (10)	1715 (60)	1709 (7)	0.0409 (39)

3. Results and discussion

3.1. Crystal structures

A necessary and sufficient condition for the formation of mixed crystals of organic molecules is similarity of the shapes and volumes of the component molecules. For the formation of true solid solutions the structures of the pure components must be isomorphous [24]. Due to the complex packing behaviour of organic molecules this situation is not often encountered and only relatively few solid-solution forming systems have been studied. The three co-monomers used for this work (DCH, DAH and ACH) meet the latter requirement and crystallized in isomorphous structures. Pertinent crystallographic data are given in Table IV. It should be noted that the structure of the unsymmetrically substituted ACH is disordered so that both the carbazolyl and anthryl side groups statistically occupy the same lattice sites. The close similarity of the crystal structures is seen on the projections on the plan plane of the monomer stacks which are shown in Fig. 1.

The packing of the diacetylene groups plays an important role in the solid state reactivity. It can be characterized by the stacking distance and the angle which the diacetylene group makes with the stacking axis. Maximal reactivity is expected when the monomers stack in a distance equal to the polymer repeat unit of 0.49 nm with an angle near to 45° [9, 10]. It can be seen that in these monomers the packing is not favourable for polymerization. Pure DCH has been found to be quite stable when irradiated with high-energy radiation. After a long induction period a phase transition occurs at which a sudden increase of the stacking distance and a change of side group packing connected with a large acceleration of the reaction is observed. This phase transition proceeds homogeneously for radiation polymerization due to nucleation phenomena at the high temperatures necessary for the reaction [14, 15, 25, 26]. In ACH and DAH the stacking distance of neighbouring monomer units is even shorter and consequently the pure Co-monomers 1b and 1c cannot be polymerized by high-energy radiation and can only be polymerized with decomposition at high temperatures near the melting points.

At 142 K DCH monomer undergoes a first-order phase transition which is characterized by a sudden decrease of the monomer stacking distance, b. Consequently this phase has been found to be completely inactive [14, 26]. Bloor [27] has reported that, at the phase transition, the crystal is deformed and that the absorption of traces of polymer present in the crystals abruptly shifts from 15100 to 18640 cm^{-1}. Larger crystals tend to fracture during the transition so only intensities for two layers could be collected for the low temperature phase. A projection of the structure is shown in Fig. 1b. Similar phase transitions could not be detected in Co-monomers 1b and 1c. Observed bond lengths and angles of the monomers are given in Fig. 2.

TABLE IIIC Final atomic parameters for C in Co-monomer 1b. Estimated standard deviations are given in parentheses

Atom	Fractional co-ordinates ($\times 10^4$)			Anisotropic temperature factors, U_{ij} ($\times 10^3$)					
	x	y	z	U_{11}	U_{22}	U_{33}	U_{12}	U_{13}	U_{23}
C (1)	9683 (9)	9206 (35)	9762 (8)	45 (9)	83 (10)	54 (9)	−14 (8)	−15 (7)	6 (8)
C (2)	9124 (10)	7969 (33)	9371 (9)	76 (11)	56 (10)	85 (12)	3 (9)	−25 (10)	11 (9)
C (3)	8368 (10)	6303 (34)	8844 (8)	83 (11)	64 (10)	65 (11)	−16 (9)	−19 (9)	4 (8)
C (4)	7765 (11)	8542 (34)	8328 (10)	59 (13)	50 (10)	106 (16)	−18 (9)	−17 (12)	−4 (10)
C (5)	6991 (11)	9884 (36)	8593 (11)	49 (11)	56 (10)	130 (18)	−13 (9)	−3 (12)	−15 (11)
C (6)	6423 (11)	11691 (37)	8094 (9)	50 (11)	77 (11)	65 (12)	0 (10)	−9 (9)	−5 (10)
C (7)	6636 (12)	12180 (38)	7320 (10)	60 (13)	80 (12)	98 (16)	2 (10)	−16 (11)	7 (11)
C (8)	7403 (11)	10914 (38)	7095 (11)	58 (12)	75 (12)	91 (15)	−17 (10)	7 (11)	−4 (11)
C (9)	7998 (11)	9077 (39)	7606 (9)	64 (12)	90 (12)	40 (10)	−9 (10)	−9 (9)	−10 (9)
C (10)	6764 (13)	9563 (48)	9336 (9)	81 (14)	148 (17)	36 (11)	−38 (14)	2 (9)	1 (11)
C (11)	5988 (14)	10998 (55)	9561 (10)	82 (15)	165 (20)	61 (14)	−48 (15)	−2 (12)	−24 (15)
C (12)	5415 (12)	12758 (46)	9033 (14)	58 (13)	114 (16)	130 (20)	−14 (12)	28 (13)	−50 (16)
C (13)	5647 (13)	13112 (46)	8355 (11)	89 (16)	112 (15)	93 (16)	18 (13)	−1 (12)	−29 (14)
C (14)	8790 (13)	7931 (40)	7321 (10)	78 (14)	101 (13)	71 (13)	−1 (11)	−6 (10)	−24 (11)
C (15)	9010 (15)	8430 (59)	6639 (15)	106 (19)	159 (22)	115 (22)	42 (17)	55 (17)	−81 (18)
C (16)	8433 (21)	10252 (68)	6146 (13)	154 (30)	187 (26)	47 (15)	−53 (22)	0 (16)	−27 (16)
C (17)	7667 (16)	11563 (53)	6384 (11)	126 (20)	140 (17)	48 (13)	−43 (16)	−24 (11)	36 (12)

TABLE IIID Final atomic parameters for the H atoms in Co-monomer 1b. Estimated standard deviations are given in parentheses. Temperature factors, B, have not been refined.

Atom	Fractional co-ordinates ($\times 10^3$)			Isotropic temperature factor, B (nm^2)
	x	y	z	
H (1)	797 (6)	484 (21)	910 (5)	0.05
H (2)	892 (6)	477 (20)	852 (5)	0.05
H (3)	612 (6)	1388 (20)	710 (5)	0.05
H (4)	714 (5)	830 (21)	898 (5)	0.05
H (5)	590 (5)	1112 (21)	1024 (5)	0.05
H (6)	489 (6)	1451 (21)	918 (5)	0.05
H (7)	524 (6)	1426 (21)	784 (4)	0.05
H (8)	905 (5)	670 (21)	761 (5)	0.05
H (9)	955 (6)	694 (20)	640 (5)	0.05
H (10)	879 (5)	1055 (20)	604 (5)	0.05
H (11)	741 (6)	252 (20)	604 (5)	0.05

3.2. Formation and polymerization of mixed crystals

Mixed crystals were grown from appropriate concentrated solutions of the monomers in DMF. Since the composition of the feed solution gradually changes during the crystallization, only the first crystals of a batch were picked. The compositions of the crystals were analysed by measuring the absorption of the anthryl side groups at 389 nm in CH_2Cl_2. The dependence of the crystal composition on the composition of the DMF solutions is plotted in Fig. 3 for the System 1a–1c.

Phase diagrams of the mixed crystals could not

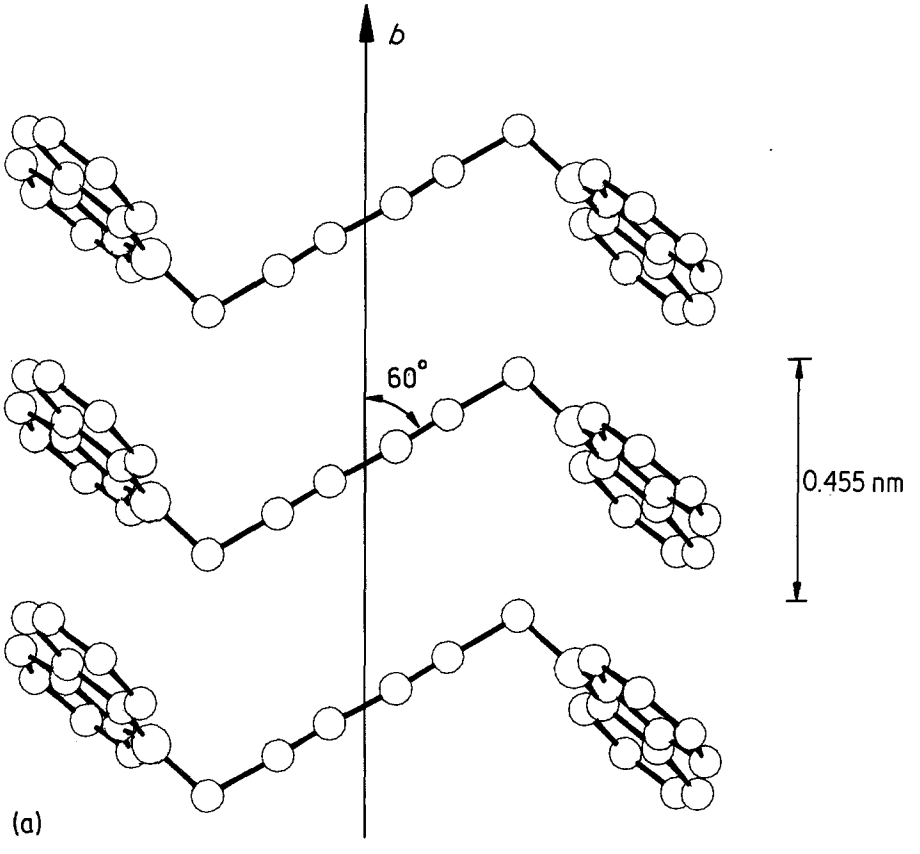

Figure 1 Projections of the monomer structures on the plane of the diacetylene stacks (a) Co-monomer 1a at room temperature, (b) Co-monomer 1a at 120 K, (c) Co-monomer 1b, (d) Co-monomer 1c.

TABLE IIIE Final atomic parameters for C and N in Co-monomer 1c. Estimated standard deviations are given in parentheses

Atom	Frictional co-ordinates ($\times 10^4$)			Anisotropic temperatures, U_{ij} ($\times 10^4$)					
	x	y	z	U_{11}	U_{22}	U_{33}	U_{12}	U_{13}	U_{23}
C (1)	9671 (3)	5735 (11)	4754 (3)	534 (25)	515 (27)	596 (27)	−5 (22)	−42 (20)	−101 (23)
C (2)	9109 (3)	7079 (11)	4332 (3)	618 (27)	499 (27)	652 (29)	62 (24)	−112 (23)	−84 (24)
C (3)	8410 (3)	8781 (12)	3838 (3)	781 (33)	564 (31)	803 (34)	88 (27)	−346 (27)	−18 (27)
C (4)	7837 (13)	6782 (47)	3295 (12)	360 (85)	607 (99)	1504 (166)	218 (70)	−98 (86)	643 (99)
C (5)	7033 (7)	5343 (23)	3623 (6)	950 (66)	468 (58)	1114 (75)	204 (52)	−282 (56)	138 (55)
C (6)	6362 (6)	3320 (19)	3121 (4)	485 (45)	491 (49)	284 (42)	186 (41)	8 (34)	7 (36)
C (7)	6558 (6)	2739 (21)	2340 (5)	530 (55)	558 (55)	487 (50)	7 (43)	−132 (38)	−68 (43)
C (8)	7394 (6)	4124 (21)	2099 (4)	488 (47)	563 (54)	281 (37)	149 (45)	156 (34)	96 (38)
C (9)	8002 (9)	6128 (24)	2572 (5)	1226 (88)	459 (61)	750 (60)	409 (64)	−363 (60)	169 (51)
C (10)	6906 (7)	5727 (25)	4256 (6)	592 (60)	882 (73)	676 (63)	157 (57)	115 (48)	155 (58)
C (11)	6056 (7)	4288 (27)	4607 (5)	616 (59)	889 (80)	766 (63)	57 (59)	−40 (47)	44 (62)
C (12)	5388 (8)	2467 (31)	4127 (7)	909 (83)	997 (95)	959 (93)	105 (76)	−264 (71)	−149 (81)
C (13)	5578 (6)	1947 (24)	3361 (5)	533 (53)	818 (69)	527 (57)	105 (52)	101 (44)	−93 (52)
C (14)	8837 (9)	7343 (28)	2379 (8)	1031 (94)	721 (76)	1491 (116)	−27 (71)	297 (84)	93 (77)
C (15)	9054 (9)	6766 (31)	1634 (7)	954 (91)	849 (96)	913 (96)	258 (78)	389 (78)	291 (80)
C (16)	8407 (9)	4840 (35)	1131 (7)	882 (91)	1155 (115)	995 (96)	−34 (88)	−242 (76)	291 (88)
C (17)	7581 (6)	3418 (25)	1345 (6)	506 (50)	805 (70)	787 (67)	26 (51)	248 (45)	107 (56)
C (24)	7983 (5)	5876 (20)	2637 (4)	372 (41)	441 (50)	613 (48)	59 (40)	−46 (35)	229 (42)
C (25)	7186 (8)	4006 (26)	2352 (5)	1023 (79)	690 (71)	411 (58)	359 (65)	−21 (53)	104 (34)
C (26)	7210 (10)	3071 (30)	1585 (8)	1389 (118)	737 (89)	1048 (97)	206 (87)	−475 (85)	118 (79)
C (27)	7995 (9)	4049 (31)	1193 (6)	1164 (90)	729 (87)	669 (73)	99 (77)	161 (65)	157 (65)
C (28)	8723 (8)	5780 (28)	1456 (7)	842 (77)	745 (78)	930 (84)	101 (70)	180 (65)	404 (68)
C (29)	8745 (6)	6842 (21)	2194 (5)	611 (55)	612 (53)	688 (56)	89 (46)	61 (43)	146 (46)
C (30)	6993 (5)	5096 (19)	3572 (4)	425 (39)	415 (47)	509 (45)	83 (36)	−29 (33)	−34 (37)
C (31)	6650 (8)	3567 (28)	2931 (7)	636 (62)	730 (74)	1373 (99)	140 (57)	−62 (65)	348 (74)
C (32)	5826 (12)	1870 (32)	3051 (10)	1650 (140)	828 (97)	1495 (144)	622 (99)	−742 (99)	−356 (99)
C (33)	5447 (7)	1948 (25)	3802 (7)	643 (64)	617 (64)	1191 (83)	75 (52)	114 (58)	−142 (62)
C (34)	5861 (8)	3448 (27)	4393 (6)	984 (83)	779 (73)	790 (76)	358 (66)	132 (63)	93 (62)
C (35)	6662 (6)	5159 (21)	4336 (5)	559 (48)	523 (52)	770 (60)	61 (44)	−80 (43)	32 (47)
N	7788 (12)	6484 (34)	3380 (7)	872 (122)	388 (77)	265 (57)	207 (71)	−175 (60)	−86 (55)

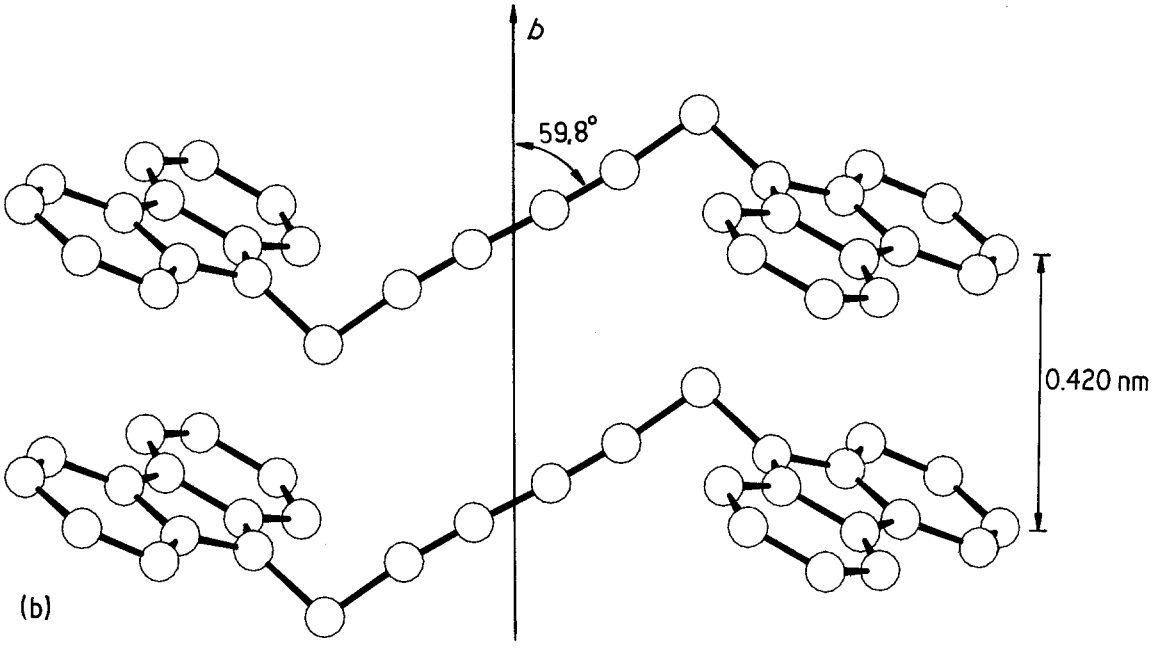

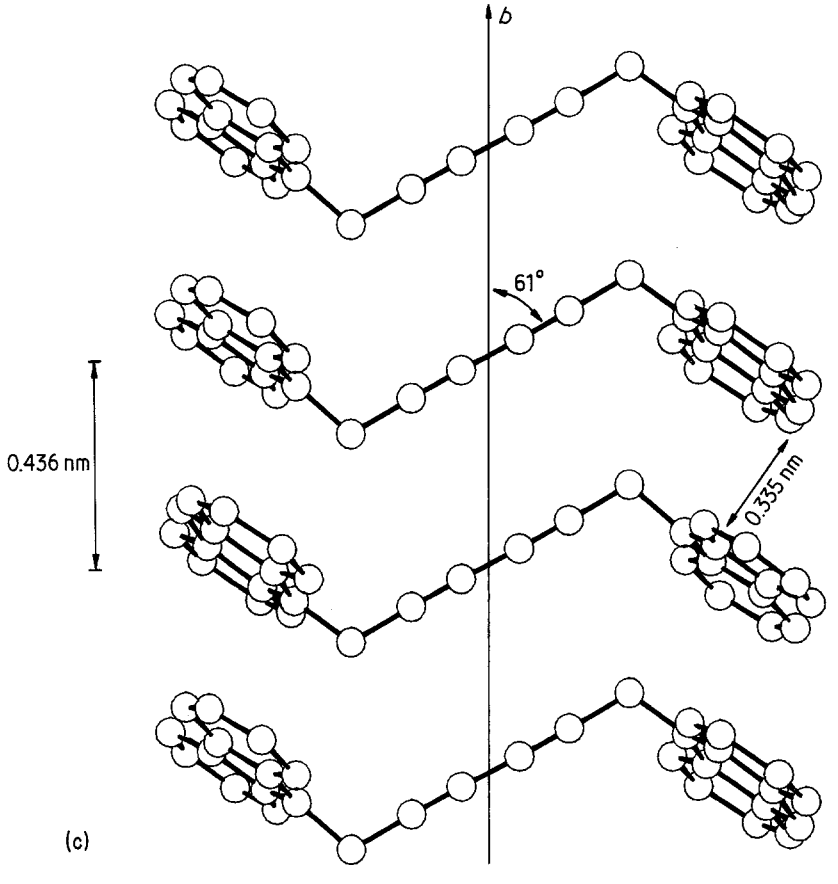

Figure 1 Continued.

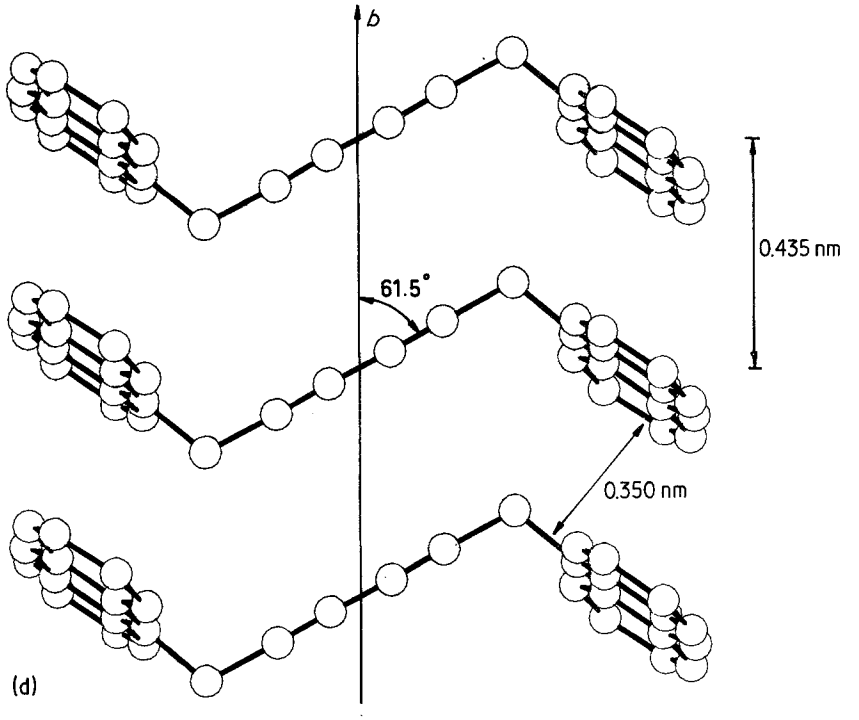

Figure 1 Continued.

be determined since even at the highest heating rates rapid polymerization above 150° C is observed. The co-crystallization diagram (Fig. 3) shows, however, that no phase separation occurs and that true substitutional solid solutions are formed over the whole concentration range. Due to the lower solubility of the monomers containing anthracene they are preferentially incorporated into the crystal. The dependence of the lattice parameters on the crystal composition is given

TABLE IIIF Final atomic parameters for the H atoms in Co-monomer 1c. Estimated standard deviations are given in parentheses. Temperature factors, B, have not been refined

Atom	Fractional co-ordinates (× 10^3)			Isotropic temperature factor, B (nm^2)
	x	y	z	
H (1)	882 (3)	1009 (15)	341 (3)	0.05
H (2)	798 (3)	993 (15)	428 (3)	0.05
H (3)	608 (5)	171 (19)	199 (4)	0.05
H (4)	740 (6)	650 (20)	486 (4)	0.05
H (5)	600 (7)	440 (17)	521 (4)	0.05
H (6)	455 (6)	159 (22)	408 (6)	0.05
H (7)	515 (8)	67 (28)	301 (5)	0.05
H (8)	933 (7)	897 (26)	267 (6)	0.05
H (9)	981 (6)	761 (17)	146 (5)	0.05
H (10)	839 (9)	425 (33)	48 (6)	0.05
H (11)	689 (6)	233 (18)	111 (5)	0.05
H (20)	669 (4)	171 (17)	128 (5)	0.05
H (21)	801 (5)	327 (19)	63 (5)	0.05
H (22)	926 (5)	635 (20)	110 (6)	0.05
H (23)	930 (6)	828 (20)	243 (5)	0.05
H (24)	547 (4)	48 (21)	263 (6)	0.05
H (25)	483 (6)	76 (27)	386 (6)	0.05
H (26)	557 (6)	331 (29)	491 (5)	0.05
H (27)	670 (5)	644 (20)	478 (6)	0.05

TABLE IV Crystallographic data (estimated standard deviations are given in parentheses)

Parameter	Co-monomer				
	1a	1a	2a*	1b	1c
Temperature (K)	300	120	300	300	300
a (× 10 nm)	13.60 (4)	13.38 (1)	12.87 (1)	14.60 (5)	14.33 (1)
b (× 10 nm)	4.55 (3)	4.20 (4)	4.91 (1)	4.35 (3)	4.36 (1)
c (× 10 nm)	17.60 (4)	18.44 (1)	17.40 (1)	17.92 (4)	18.00 (1)
(°)	94.0 (5)	92.0 (5)	108.0 (2)	97.0 (5)	96.1 (2)
D_x (Mg m^{-3})	1.25	1.31	1.30	1.26	1.25
Z	4	4	4	4	4
Space group	$P2_1/c$	$P2_1/c$	$P2_1/c$	$P2_1/c$	$P2_1/c$

*From [25].

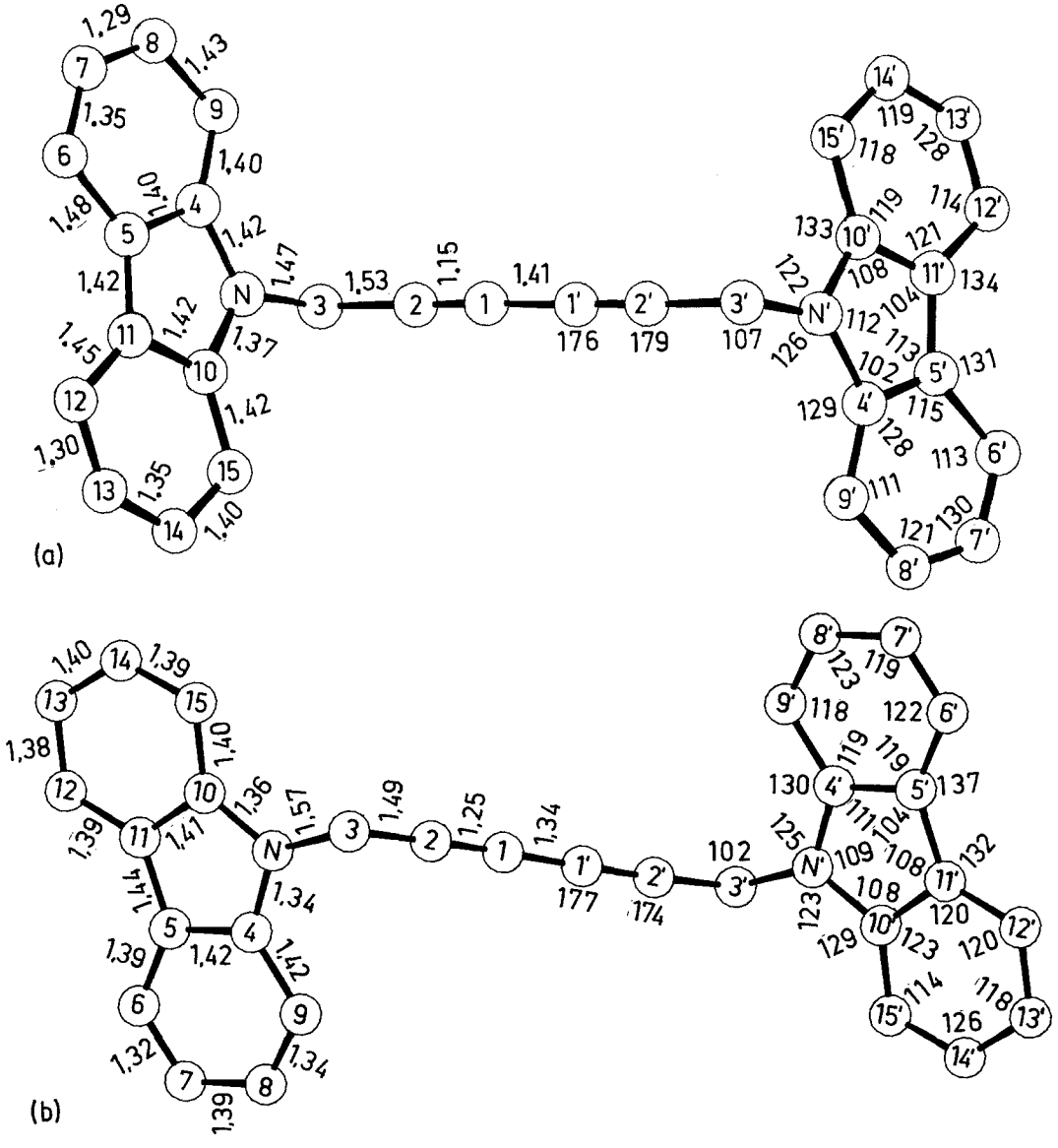

Figure 2 Observed bond lengths (× 10 mm) and angles (°) for (a) Co-monomer la at room temperature, (b) Co-monomer 1a at 120 K, (c) Co-monomer 1b, (d) Co-monomer 1c. Estimated standard deviations for bond lengths are of the order of 2 × 10^{-3} nm for Co-monomer 1a and 1 × 10^{-3} nm for Co-monomers 1b and 1c, for bond angles of 1 to 2°.

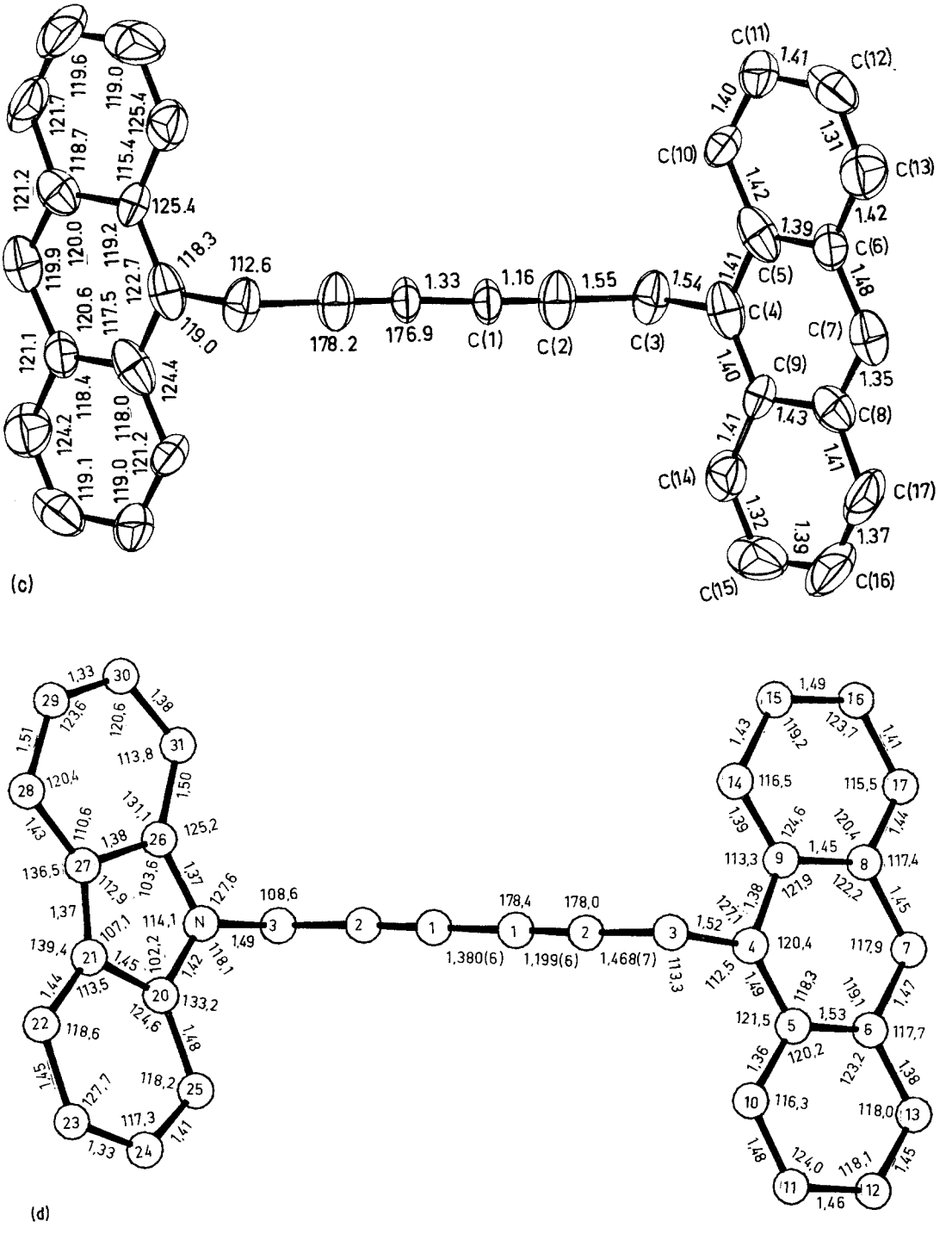

Figure 2 Continued.

for System 1a–1c in Fig. 4. The lattice dimensions change continuously and no double reflections due to phase separation could be detected nor any decrease of the intensity of higher order reflections due to disorder.

Dosage conversion curves for the gamma-ray polymerization of a series of mixed crystals are plotted in Fig. 5. They are characterized by a long induction period followed by a rapid reaction. At the onset of the fast polymerization regime a

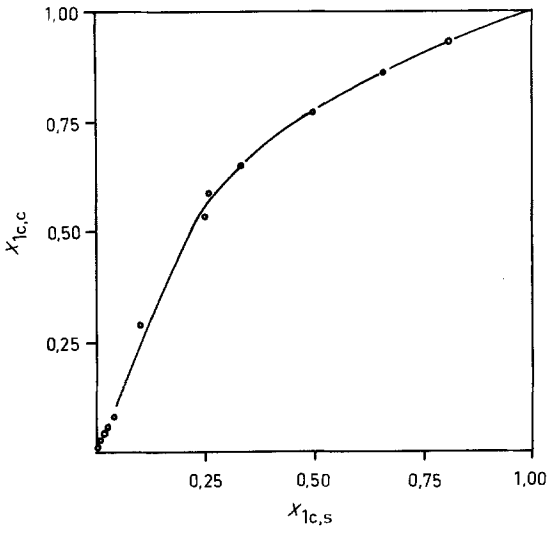

Figure 3 Dependence of mixed crystal composition on the composition of the DMF feed solution. $x_{1c,s}$, $x_{1c,c}$ represent mole fractions of Co-monomer 1c in DMF and crystal, respectively.

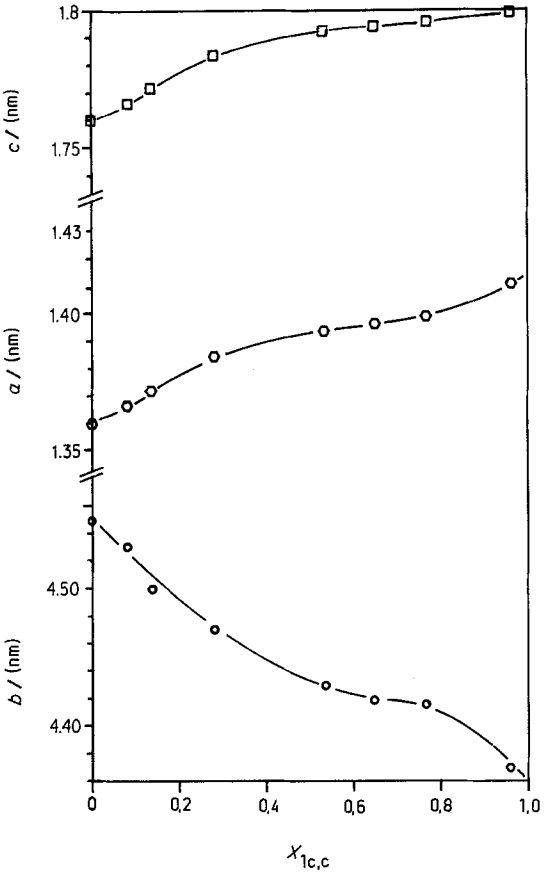

Figure 4 Dependence of the lattice parameters on the composition of the mixed crystals.

phase transition occurs which has been studied for pure DCH using structure analysis and Brillouin scattering [26]. It is interesting to note that quite small amounts of the anthracene containing co-monomers have a drastic effect on the polymerization kinetics which cannot be understood by the simple geometric approach of the least-motion principle [10]. In crystals containing 2 wt% of Co-monomer 1c or 1 wt% of Co-monomer 1b the induction period is more than doubled. Analysis of the residual monomer mixture which can be extracted from partially polymerized crystals shows that, regardless of the conversion, the composition of the polymer and the residual monomers is always equal to the composition of the original monomer crystal. In this concentration range the lattice parameters remain virtually constant so that the consideration of the monomer packing, which has been used successfully to explain differences of reactivity between different monomers and crystal modifications, is not able to predict this drastic doping effect on the polymerization rate [9–12].

Similar inhibiting effects of small amounts of Co-monomers 1b and 1c can also be observed in the photopolymerization of mixed crystals if the crystals are irradiated within the absorption bands of the triple bond system (250 nm) or the carbazole group (350 nm). In the photopolymerization the polymer is not distributed equally in the crystal but is formed preferentially at the surface, and acts as a filter hindering the reaction inside the crystal. Therefore the reaction kinetics can be followed qualitatively by irradiation of small crystals on the stage of an u.v. microscope with simultaneous determination of the optical density arising from the polymer [28]. When the crystals were irradiated at 400 nm within the adsorption band of the anthryl groups, however, the opposite effect of photosensitation by the co-monomer was observed. For example, a crystal containing 1 wt% of Co-monomer 1c polymerized four times faster than a pure DCH crystal under otherwise identical conditions.

3.3. Energy transfer and polymerization

The experimental facts that quenching and photosensitation by the co-monomer units occurs in different wavelength ranges can be understood by the mechanism of energy transfer which plays an important role in the solid-state polymerization

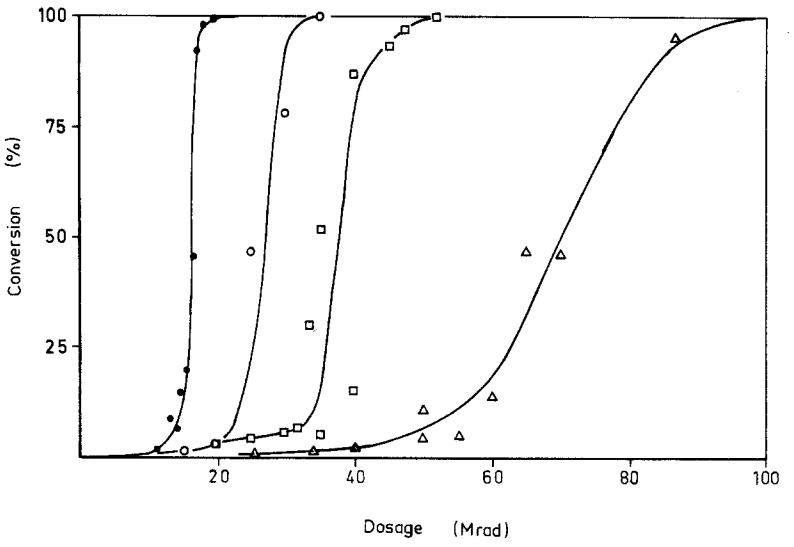

Figure 5 Dosage conversion curves for the gamma-ray polymerization of mixed crystals. •: pure Co-monomer 1a, ○: $x_{1c,c} = 0.011$, □: $x_{1c,c} = 0.022$, △: $x_{1c,c} = 0.055$.

of diacetylenes. Analyses of the isotope effects observed in the polymerization [29] and of the kinetic data obtained in flash photochemical experiments [30] have shown that the rate determining factor for the reaction is the energy transport to reaction sites.

This can be described as a random walk of excited states to randomly distributed reaction centres, which can be pictured as crystallographic defects or sites built into the monomer lattice by the polymerization itself like, for example, chain ends. In the mixed crystals the anthracene groups act as traps for the excited states. It must be assumed that only a small fraction of the energy trapped at the co-monomer side groups can be transferred to the triple-bond system, and most of it is emitted as fluorescence. This explains why traces of the co-monomers effectively quench the polymerization as most of the energy necessary for the reaction is emitted before it reaches the reaction sites. If the mixed crystals are irradiated, however, at 400 nm, where only the anthryl groups absorb, the small energy fraction which is transferred to the diacetylene group is responsible for the observed photosensitation effect [31, 32].

Pure DCH shows four broad fluorescence bands at 27360, 24780, 23360 and 22120 cm^{-1} [15, 19]. This fluorescence is completely quenched when traces of Co-monomers 1b or 1c are present, and instead fluorescence from the anthryl groups is

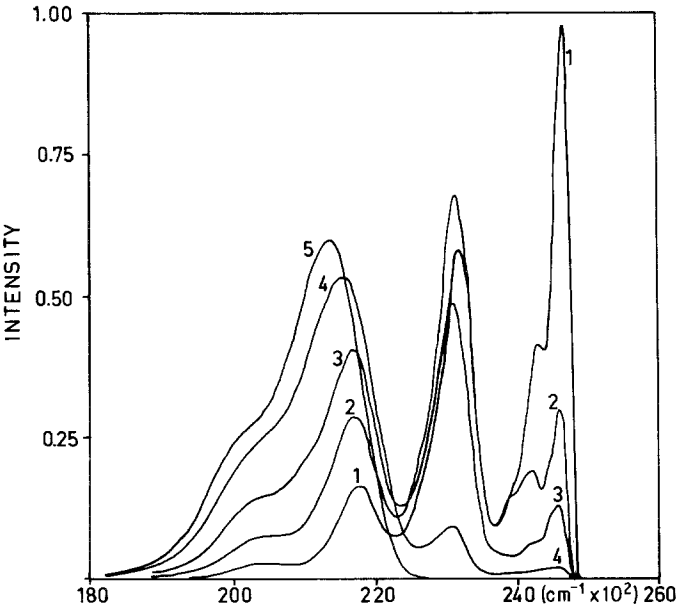

Figure 6 Fluorescence spectra of mixed crystals recorded at 4.2 K. 1: $x_{1c,c} = 0.0026$, 2: $x_{1c,c} = 0.019$, 3: $x_{1c,c} = 0.088$, 4: $x_{1c,c} = 0.144$, 5: pure Co-monomer 1c.

observed. With small concentrations of co-monomer the rather sharp spectra of isolated anthracene units are observed, which, with increasing co-monomer content, gradually shift toward the broad fluorescence typical for pure DAH or ACH. This behaviour is shown in Fig. 6 and indicates that with increasing concentration anthracene clusters are formed.

The question of how the co-monomer units are distributed in the crystal and what are the resulting co-polymer statistics cannot be answered unambiguously on the basis of the experimental data. However, the absence of any phase separation, the formation of true solid solutions and the fact that the co-monomer units are incorporated into the polymer according to the composition of the parent crystal indicate that there is a statistical distribution. Due to the limited reactivity of mixed crystals with higher co-monomer concentrations and to the poor solubility of the polymers, which makes the analysis of the polymer impossible, there is no information on whether the co-monomer acts as a site where the reaction is preferentially terminated. Further work on the influence of isostructural doping on reactivity, molecular weight and molecular-weight distribution is in progress with a series of co-monomers which form soluble diacetylene polymers [33].

Acknowledgement

Financial support by Stiftung Volkswagenwerk is gratefully acknowledged.

References

1. G. WEGNER, *Makromol. Chem.* **154** (1972) 35.
2. *Idem,* in "Molecular Metals", edited by W. E. Hatfield (Plenum Press, New York, 1979) p. 209.
3. G. C. STEVENS and D. BLOOR, *Chem. Phys. Lett.* **40** (1976) 37.
4. H. EICHELE, M. SCHWOERER, C. BUBECK and H. SIXL, *ibid.* **53** (1978) 342.
5. C. BUBECK, H. SIXL and H. C. WOLF, *Chem. Phys.* **32** (1978) 231.
6. R. HUBER, M. SCHWOERER, C. BUBECK and H. SIXL, *Chem. Phys. Lett.* **53** (1978) 35.
7. H. NIEDERWALD, H. EICHELE and M. SCHWOERER, *ibid.* **72** (1980) 242.
8. V. ENKELMANN and G. WEGNER, *Angew. Chem.* **89** (1977) 432.
9. V. ENKELMANN and H. J. GRAF, *Acta Cryst. B* **34** (1978) 3715.
10. R. H. BAUGHMAN, *J. Polymer Sci. Polymer Phys. Ed.* **12** (1974) 1511.
11. V. ENKELMANN, *Makromol. Chem.* **179** (1978) 2811.
12. *Idem, J. Mater. Sci.* **15** (1980) 951.
13. D. BLOOR, D. J. ANDO, R. L. WILLIAMS and M. MOTEVALLI, Abstracts of the 9th Molecular Crystal Symposium, Mittelberg, Austria, 1980.
14. V. ENKELMANN and G. SCHLEIER, *Polymer Prepr. Div. Polymer Chem. Amer. Chem. Soc.* **19** (1978) 142.
15. V. ENKELMANN, G. SCHLEIER, G. WEGNER, H. EICHELE and M. SCHWOERER, *Chem. Phys. Lett.* **52** (1977) 314.
16. K. C. YEE and R. R. CHANCE, *J. Polymer Sci. Polymer Phys. Ed.* **16** (1978) 431.
17. R. SKOWRONSKI and W. CHODKIEWICZ, *Comp. Rend. I* **251** (1960) 547.
18. G. SCHLEIER, PhD thesis, Freiburg University (1980).
19. H. EICHELE, PhD thesis, Bayreuth University (1978).
20. J. P. DECLERCQ, G. GERMAIN, P. MAIN and M. M. WOOLFSON, *Acta Cryst. A* **29** (1973) 231.
21. J. M. STEWART, P. A. MACHIN, C. DICKINSON, H. L. AMMON, H. HECK and H. FLACK, "The XRAY system – version of March 1976", Technical Report number TR-446 (Computer Science Center, Univ. of Maryland, Maryland, 1976).
22. C. A. MACGILLAVRY and G. D. RIECK (EDS), "International Tables for X-ray Crystallography" Vol. III, 2nd edition (Kynoch Press, Birmingham, 1968).
23. R. F. STEWART, E. R. DAVIDSON and W. T. SIMPSON, *J. Chem. Phys.* **42** (1965) 3175.
24. A. I. KITAIGORODSKII, "Molecular Crystals and Molecules" (Academic Press, New York, 1973) p. 94.
25. P. A. APGAR and K. C. YEE, *Acta Cryst. B* **34** (1978) 957.
26. V. ENKELMANN, R. J. LEYRER, G. SCHLEIER and G. WEGNER, *J. Mater. Sci.* **15** (1980) 168.
27. R. J. KENNEDY, I. F. CHALMERS and D. BLOOR, *Makromol. Chem. Rapid Comm.* **1** (1980) 168.
28. G. WEGNER, *Pure Appl. Chem.* **49** (1977) 443.
29. C. KRÖHNKE, V. ENKELMANN and G. WEGNER, *Chem. Phys. Lett.* **71** (1980) 38.
30. R. J. LEYRER and G. WEGNER, *Ber. Bunsenges. Phys. Chem.* **83** (1979) 470.
31. R. J. LEYRER, PhD thesis, Freiburg University (1979).
32. B. TIEKE and G. WEGNER, *Makromol. Chem.* **179** (1978) 2573.
33. G. WENZ, V. ENKELMANN and G. WEGNER, unpublished work.

Received 5 May
and accepted 15 July 1981